New isotope ^{80}Y, and the decays of ^{79}Sr, ^{81}Y, and ^{82}Y

C. J. Lister,* P. E. Haustein, D. E. Alburger, and J. W. Olness
Brookhaven National Laboratory, Upton, New York 11973
(Received 28 January 1981)

The helium-jet recoil transfer technique has been used to study the decays of ^{79}Sr, ^{80}Y, ^{81}Y, and ^{82}Y, produced by ^{58}Ni(^{24}Mg,2pn), ^{58}Ni(^{24}Mg,pn), ^{58}Ni(^{25}Mg,pn), and ^{60}Ni(^{24}Mg,pn) reactions, respectively. Decay properties of these four radioactivities have been deduced from the analysis of extensive singles and multiparameter spectroscopic measurements. The low lying level structure of ^{80}Sr, as revealed by the decay of ^{80}Y, can be reproduced through calculations of the interacting-boson-approximation model which place ^{80}Sr at or near the O(6) limit. Positron endpoint measurements [deduced from (β,γ) coincidence studies] have been used to determine decay energies for each of these nuclides. Nuclidic mass excesses inferred from these data show progressively larger deviations from the predictions of currently available mass models for the more neutron-deficient Y isotopes as the $N=Z$ line is approached. It is suggested that this may reflect the influence of nuclear deformation of these isotopes on the mass surface in the vicinity of $N=Z=40$.

[RADIOACTIVITY ^{79}Sr from ^{58}Ni(^{24}Mg, 2pn); ^{80}Y from ^{58}Ni(^{24}Mg,pn); ^{81}Y from ^{58}Ni(^{25}Mg,pn); ^{82}Y from ^{60}Ni(^{24}Mg,pn); measured $T_{1/2}$, $\sigma(E)$, E_γ, E_x, E_β, I_γ, I_x, I_β, (γ,γ,t), (X,γ,t), (β,γ,t) coincidences; deduced levels, J^π, Q_β, mass excess, logft; He-jet system, enriched targets, Ge(Li), Ge and plastic detectors; comparison with mass predictions.]

I. INTRODUCTION

Spectroscopic studies of nuclei which lie far from the line of β stability permit tests of the detailed predictions of nuclear structure theories and provide a means for delineating the nature of the nuclidic mass surface in these regions, thereby yielding additional input for the refinement of models of mass systematics. In particular, nuclei which lie on or near the $N=Z$ line are expected to provide some of the most stringent tests of these theories.[1] Nuclei in this region are expected to highlight the influences of a variety of nuclear structure features which affect both the nature of the mass surface and the character of the excited state spectrum of these nuclei. These include isospin effects, the influences of nuclear shells on binding energies, single particle versus collective phenomena, Coulomb energy considerations, symmetry effects, and the role of nuclear deformation in regions of an unusual N/Z ratio.

One region of particular interest for studies of this type centers around the nuclei near ^{80}Zr. This mass region represents the one in which heavy-ion reactions can be employed to produce the heaviest compound nuclei with $N=Z$. It is also a region in which it is thought that nuclear deformation is strongly coupled to neutron and proton occupancy of those orbitals which are partially filled between the shell closures at 28 and 50 nucleons. Evidence[2] for large oblate deformation for these nuclei comes from the observation of rapid changes which occur in the excitation energy of the first excited 2^+ level in even-even nuclei in this region.

Numerous earlier studies[3] of these nuclei concentrated on off-line measurements using radioactive sources produced by a variety of heavy-ion reactions on targets of normal isotopic distribution. In some cases, chemical separations and β-ray counting were performed to aid the identification of the atomic number of the product nuclei and to infer parent-daughter relationships. Frequently the production reactions were initiated with entrance channel energies that were well above the Coulomb barrier; isotopic assignments were nevertheless made in many cases with the assumption that the exit channels were dominated by (HI, xn) pathways.

Evaporation calculations performed with several presently available codes indicate, however, that at the beam energies used in the earlier studies, both proton and α-particle emission compete freely with neutron evaporation. In-beam γ-ray measurements of Nolte *et al.*[3] and others[4] confirm these predictions. These facts, the conflicting reports on the decay properties of ^{79}Sr, and the reported observation of anomalously long half-lives for nuclides such as ^{78}Sr, whose reported half-life is at variance with its reported predicted high decay energy, led to a decision to reinvestigate the radioactive decays of isotopes in this mass region.

Shortly after the start of the present study, a new isotope, ^{80}Y, $T_{1/2}=34$ s, was observed. A preliminary report of the ^{80}Y decay, as well as that of ^{79}Sr and ^{82}Y has appeared.[5] Nearly simultaneously, a group[6] at Florida State University

reported on their reinvestigation of the ^{79}Sr decay, and a group[7] at Orsay published decay energy measurements of ^{79}Sr and ^{82}Y which were in agreement with the BNL results.

This paper reports detailed decay scheme information for ^{79}Sr and $^{80-82}$Y, including the results of (β,γ) coincidence measurements used to determine total decay energies. These results and similar data for neighboring nuclides provide the first definitive checks of model predictions for masses in the region of $N \approx Z \approx 40$.

II. EXPERIMENTAL

A. Radiochemical studies

The first reported observation of the ^{78}Sr and ^{79}Sr decays was by Bilge and Boswell.[8,9] They employed beams of 160-MeV ^{16}O on a natural Zn target to produce several Sr compound nuclei, which they chemically separated from the target; the decay of these sources was then followed using NaI(Tl) detectors. The principal reaction mechanism was assumed to be $(^{16}O, xn)$, and so the observation of 31- and 8.1-min half-lives followed by the growth of Rb activities led to the assignment of these isotopes to ^{78}Sr and ^{79}Sr, respectively. When a source was counted with a Ge(Li) detector, the γ-ray spectrum was reported to contain seven gamma lines (116, 166, 189, 256, 444, 560, and 611 keV) which decayed with half-lives of 8.3 to 9.5 min. These were attributed to the ^{79}Sr decay.

More recent heavy-ion studies have indicated conflicting results for ^{79}Sr. Ladenbauer-Bellis *et al.*[10] and Doran and Blann[4] reported observing this decay, the former indicating a γ ray of energy 105.4 ± 0.2 keV with $T_{1/2} = 4.4 \pm 0.2$ min [following ^{69}Ga$(^{14}N, 4n)^{79}$Sr], while the latter reported γ rays of 105.0 ± 0.5, 134.9 ± 0.2, and 219.1 ± 0.2 keV and $T_{1/2} = 1.9 \pm 0.5$ min [following ^{50}Cr$(^{32}S, 2pn)^{79}$Sr]. In an attempt to resolve these conflicting reports we repeated the ^{16}O + (natural) Zn study of Bilge and Boswell.

A 0.025-mm thick natural Zn target was irradiated for 55 min by a 70-MeV ^{16}O beam (50 particle nA). This energy was chosen to optimize three and four particle emission required to populate the mass 78 and 79 chains. The irradiation duration would ensure the nearly complete saturation of the 31-min ^{78}Sr activity reported by Bilge and Boswell.[8] The target was then dissolved in 90% nitric acid. Carriers were added for Br, Rb, and Sr. Cooling the target solution to 0 °C precipitated the Sr. After decanting the supernate, the Sr was washed and reprecipitated several times. The chemical procedure required about 20 min following the end of irradiation, and the first count began 4 min after the end of the chemistry. Gamma-ray spectra were accumulated in time bins varying from 5 min to 1 h for the next 80 h. Decays from the $A = 80-83$ chains were all observed, but no evidence for the ^{78}Sr or ^{79}Sr activities was obtained.

One of two conclusions may be drawn from these observations: (1) Either the production cross section for ^{78,79}Sr from this reaction is significantly less than 1 mb, so undetectable amounts of the isotopes are produced; or (2) one must conclude that the lifetimes are sufficiently short so that most of these isotopes decayed before counting commenced. Certainly this would be the case if $T_{1/2} \sim 2$ min because the amount of decay between the end of the irradiation and the start of counting would be greater than a factor of 10^3, and activities produced at the 100 mb level would not be observed. Evaporation calculations using the CASCADE code[11] favor this latter hypothesis. Our measurements (and those in Refs. 6 and 7) of the decay of ^{79}Sr reported below confirm that this is the case for $A = 79$, and grave doubt is cast on the assignment[8] of $T_{1/2} = 31$ min for the half-life of ^{78}Sr.

B. Helium-jet studies

Radioactive sources of ^{79}Sr and $^{80-82}$Y were prepared by heavy-ion reactions with beams from the BNL Tandem Van de Graaff facility. Table I lists the projectile and/or target combinations which were employed and the beam energies which were used. For each product activity of interest, the excitation energy of the intermediate compound nucleus was generally kept low and carefully adjusted to maximize the yield of the desired product. Evaporation calculations were performed to select optimal energies and in some cases "in-beam" γ-ray measurements were also made to check the predictions of the excitation functions from the evaporation calculations, and as a cross confirmation of isotopic assignments in those cases where a particular γ-ray transition arose from both "out of beam" radioactive decays and also from in-beam deexcitation of evaporation residues produced directly in the heavy-ion reaction.

The helium-jet recoil transfer technique was employed as a means of continuously preparing essentially massless radioactive sources for either γ-ray or β-ray spectroscopy. A schematic of the experimental apparatus is shown in Fig. 1. Heavy-ion beams were collimated to 1 mm^2 and focused onto the targets, which typically had thicknesses of 0.6 to 2.5 mg/cm^2. Initial experiments used natural Ni as both target and vacuum

TABLE I. Projectile-target combinations and beam energies used to produce radioactive sources of ^{79}Sr and $^{80-83}$Y; summary of measurements.

Isotope	Reaction	Beam energy (MeV) Range	Optimum	Measurements
^{79}Sr	^{58}Ni(^{24}Mg, $2pn$)^{79}Sr	75–105	(90)	$T_{1/2}$, E_γ, I_γ, γ-γ, X-γ, β-γ
	^{60}Ni(^{24}Mg, αn)^{79}Sr	75–105	(95)	$T_{1/2}$, E_γ, I_γ
^{80}Y	^{58}Ni(^{24}Mg, pn)^{80}Y	75–105	(85)	$T_{1/2}$, E_γ, I_γ, γ-γ, X-γ, β-γ
	^{58}Ni(^{25}Mg, $p2n$)^{80}Y	91–110	(95)	E_γ, I_γ
	^{58}Ni(^{28}Si, αpn)^{80}Y	90–110	(110)	E_γ, I_γ
^{81}Y	^{58}Ni(^{25}Mg, pn)^{81}Y	91–110	(95)	$T_{1/2}$, E_γ, I_γ, γ-γ, X-γ
	^{58}Ni(^{28}Si, αp)^{81}Y	90–110	(105)	$T_{1/2}$, E_γ, I_γ, β-γ
	^{58}Ni(^{29}Si, αpn)^{81}Y	110	(110)	E_γ, I_γ
^{82}Y	^{60}Ni(^{24}Mg, pn)^{82}Y	75–105	(90)	$T_{1/2}$, E_γ, I_γ, γ-γ, β-γ
	^{60}Ni(^{28}Si, αpn)^{82}Y	90–110	(110)	E_γ, I_γ, β-γ
^{83}Y	^{60}Ni(^{28}Si, αp)^{83}Y	90–110	(105)	$T_{1/2}$, E_γ, I_γ, γ-γ, β-γ

window. Later experiments with enriched Ni (>96%, 1.5–2.5 mg/cm^2) isotopes used a 4-mg/cm^2 thick Ta entrance window. Recoil products which emerged from the target were thermalized in helium to which small admixtures of water vapor and isopentyl alcohol had been added (1 : 1 mixture) by a bubbler system to improve transport efficiency. The recoils were collected into a multiple capillary bundle which consisted of six stainless steel needles. The lengths of the needles were selected to span the distribution of recoil ranges of the evaporation residues. The helium

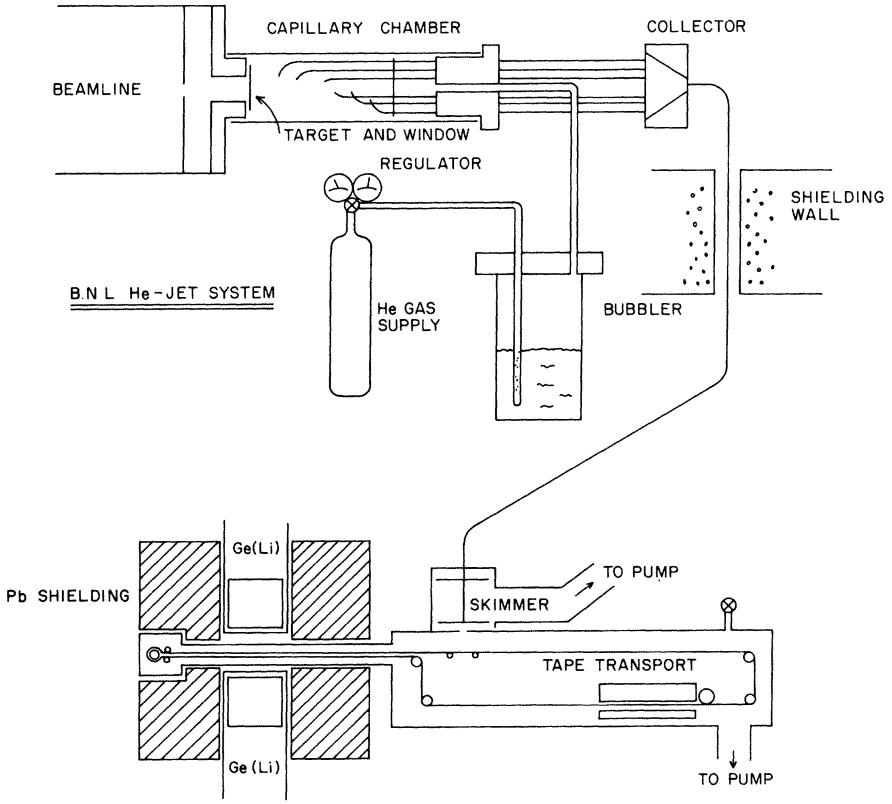

FIG. 1. A schematic view of the helium-jet transport system as used in a γ-γ coincidence experiment. The target chamber and tape system are not drawn to scale.

flow from the capillary bundle was combined into a single capillary of the same size (1-mm i.d.) and the resulting flow was directed ~5 m through a shielding wall from the irradiation station to a counting area by means of polyethylene surgical tubing. At the counting station, which has been described previously,[12] the recoil products were deposited onto an aluminized Mylar tape loop. The tape could be advanced, under computer control, to shuttle the radioactive sources from the deposition region to a counting region. The time periods during which the tape was stopped for counting of one source and collection of the next could be varied so that the collection and counting system could be "tuned" to enhance the observation of isotopes with particular half-lives. Interferences from long lived daughter activities were effectively eliminated by this periodic removal of the sources from the detector area after each collection and counting period ended.

A variety of spectroscopic measurements were made using Ge(Li), intrinsic Ge, and plastic detectors. Conventional electronics were used and spectra were accumulated using the BNL Σ-7 computer. Both singles and coincidence data were collected, the latter being four parameter data consisting of two analog signals, their relative time, and the time of the coincidence event after the last tape shuttle. The coincidence time-to-amplitude converter (TAC) spectra were accumulated to search for isomeric states in the 10 ns–1 μs time range. The scaler output, proportional to time-from-shuttle, was included to permit the generation of decay curves. These multiparameter data were sorted in a variety of ways to examine the coincidence relationships between transitions, and the half-lives of the several different radioactivities encountered. As a systematic way of determining the total decay energies of the isotopes observed through the measurement of positron end points, a 6.4 cm diameter plastic detector replaced one of the Ge(Li) detectors. This detector was calibrated using the procedure of Davids *et al.*[13] in which a "shape function" was determined from the positron spectra of several standards, e.g., ^{27}Si or ^{58}Cu produced by the (p,n) reaction on Al and Ni targets, respectively. Representative positron spectra from these calibration sources are shown in Fig. 2. The inset shows the linear dependence of the stretch factor α on the positron end point. Errors attributed to measurements of this type were estimated from the nonlinear least squares shape fitting procedure, the statistical quality of both the calibration and "unknown" spectra, and the linearity and reproducibility of the detector response. Where several different (β,γ) gates were used in a particular decay, the error in the resultant end point (and the total decay energy derived from it) reflects the composite of the individual determinations and their errors.

III. SPECTROSCOPIC RESULTS

A. ^{79}Sr→^{79}Rb decay

The weighted average decay half-life of 2.30 ± 0.10 min for the 105-, 141-, and 219-keV γ rays of the ^{79}Sr→^{79}Rb decay has already been reported[5,14] by our group. This result has been confirmed by other recent half-life measurements of 2.52 min (Florida State University)[6] and 1.9 min (Orsay).[7] The ground-state spin of ^{79}Rb is known to be $J=\frac{5}{2}$. Conflicting parity assignments have been made which are discussed in Sec. IV; in this section we have assumed that the parity is not known. At the start of the present work no excited states were known in ^{79}Rb. Recently a sequence of positive parity states has been reported by Clements[15] *et al.* which appear to be a decoupled band based on a $J^\pi=\frac{9}{2}^+$ state at 96.8 keV.

Six new levels in ^{79}Rb have been found in the present study. A 39-keV transition reported by the FSU group[6] has been observed in our X-γ coincidence studies, and has been found to be the decay of an isomeric level in ^{79}Rb that has a half-life of 23 ± 1 ns. This lifetime was measured by electronic timing, detecting prompt 511 keV annihilation quanta from positron decay in a Ge(Li) detector and delayed 39-keV γ rays in an intrinsic planar Ge detector. The resulting time spectrum is shown in Fig. 3. The prompt coincidence time peak had a full width at half maximum (FWHM) of 7 ns, and this value has been used as an upper limit for the half-lives of the other levels in ^{79}Rb as no centroid shifts or decay tails were observed for transitions from these other levels. A representative low energy γ-ray spectrum from the decay of ^{79}Sr is shown in the lower panel of Fig. 4.

The X-γ coincidence studies also showed the 39-keV transition to be highly converted, as its presence was always accompanied by 13.4- and 15.0-keV Rb $K\alpha$ and $K\beta$ x rays. Intensity measurements from the 105- and 135-keV windows resulted in an estimate of $\alpha_K^{39}=4.3\pm0.1$. However, this result did not take into account conversion x rays from transitions placed higher in the level scheme. A reanalysis was made under the extreme assumption that all higher lines of unknown multipolarity were of an $M2$ type; this reduces α_K to 4.0 ± 0.1, so consequently a value of $\alpha_K^{39}=4.1\pm0.3$ was adopted. This value is larger than that expected[16] for either $E1$ or $M1$ dipole decays, while considerably smaller than that expected for

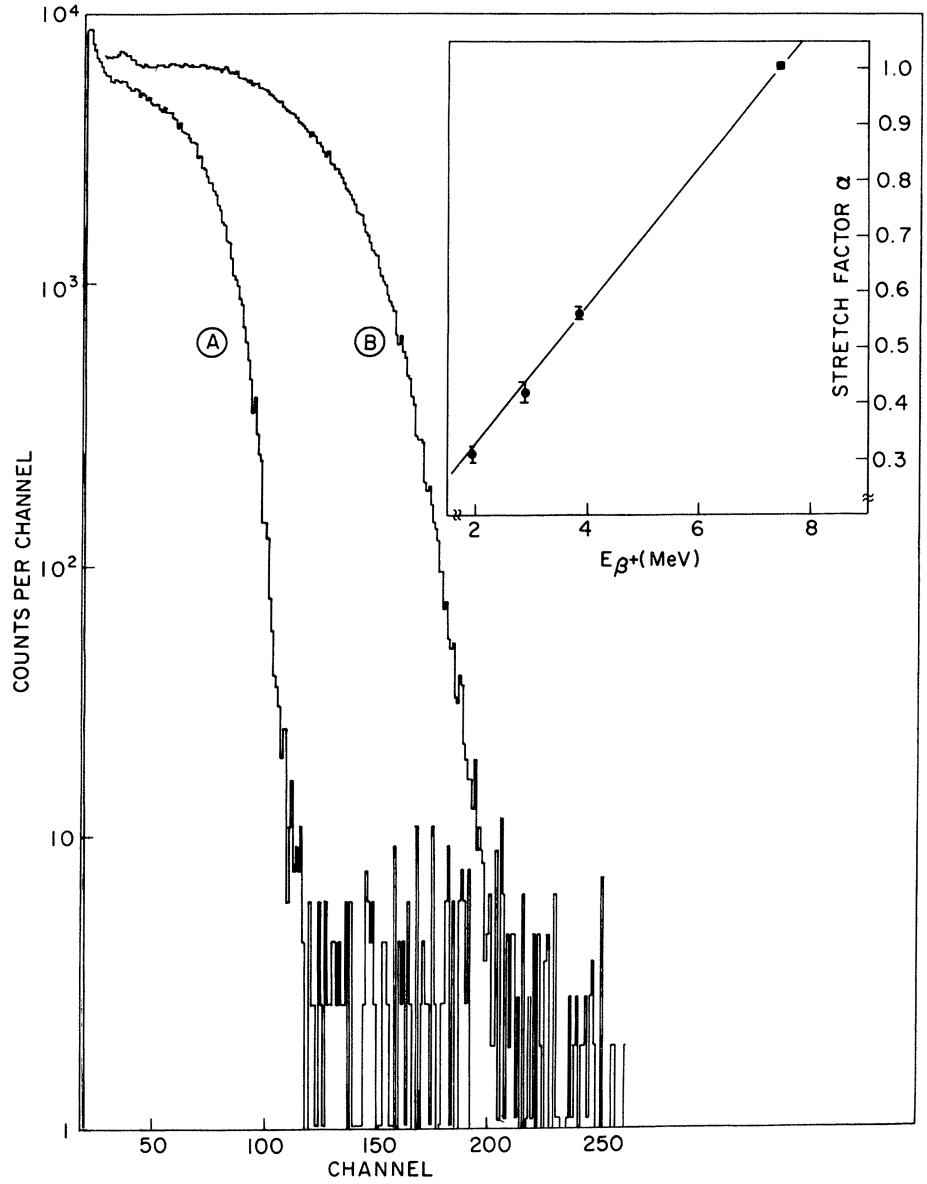

FIG. 2. Typical positron spectra used for calibrating the plastic detector. Spectrum A from $^{27}\mathrm{Al}(p,n)^{27}\mathrm{Si}$, $E_{\beta^+}^{\max}$ =3850 keV; spectrum B from $^{58}\mathrm{Ni}(p,n)^{58}\mathrm{Cu}$, $E_{\beta^+}^{\max}$=7439 keV. The insert shows the linear dependence of the stretch factor α on the positron end point energy.

$L=2$ transitions. In addition, the lifetime measurement precludes the possibility of a significant $M2$ contribution, so the multipolarity of this decay can only be an $E2/M1$ mixture with $|\delta|=0.32 \pm 0.02$.

The conversion coefficient measured for the 105-keV transition was $\alpha_K^{105}=0.56\pm0.24$ which, taken with the lifetime limit $T_{1/2}\leq 7$ ns, indicated a further $E2/M1$ decay with $|\delta|=1.2\pm0.5$. Coincidence windows set on 141- and 219-keV γ rays revealed evidence of a crossover 144-keV ground state decay. However, as the 39- and 105-keV γ rays were very intense, a large $(47\pm10\%)$ correction to the strength of this branch was required for γ-ray summing in the detectors. This effect was directly determined by measuring the intensity of the (39+141)- and (39+219)-keV sum peaks, which have no true crossover combination. After correction, the ground state γ branch was inferred to be $5.0\pm2.0\%$. Such a small crossover branch is consistent with an $E2$ transition competing against $E2/M1$ decays. Although it was not rigorously established, the 144-keV decay was assumed to be an $E2$ transition in calculating the adopted

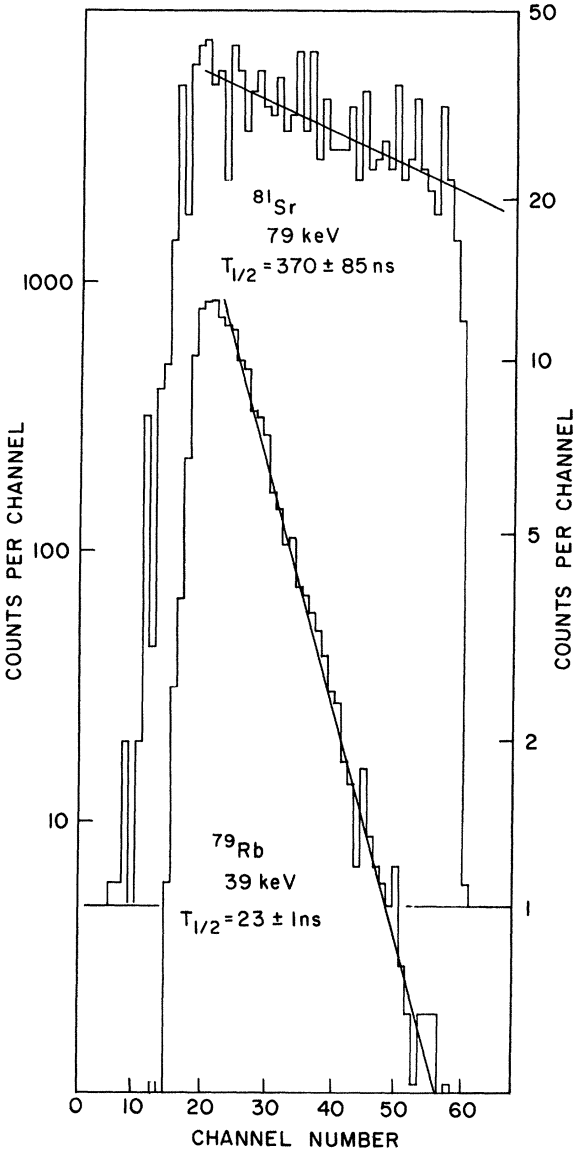

FIG. 3. LEPS-Ge(Li) coincident time distributions revealing isomeric levels at 39 keV in ^{79}Rb and at 79 keV in ^{81}Sr. The lower panel is the time distribution of 39–511 keV coincidences in ^{79}Rb, while the upper is that for 79–124 keV coincidences in ^{81}Sr.

ground state branch from the 144-keV level as 6.0 ± 2.0%. Two spin sequences are allowed by these data $J=\frac{5}{2}$, $\frac{7}{2}$, and $\frac{9}{2}$ for the ground, 39-keV, and 144-keV states, or $J=\frac{5}{2}$, $\frac{3}{2}$, $\frac{1}{2}$. However, the ^{79}Sr β^+ decay does not populate the known[15] ($\frac{9}{2}^+$) state at 97 keV and so would not be expected to populate other $J=\frac{9}{2}$ states. Further, no decays are seen between the 97-keV state and the 0-, 39-, and 144-keV levels, either in-beam or during radioactivity studies. Consequently the $J=\frac{5}{2}$, $\frac{3}{2}$, $\frac{1}{2}$ sequence is strongly favored.

The two higher levels at 285 and 363 keV were both found to have significant decays to the levels at 39 ($J^\pi=\frac{3}{2}$) and 144 ($J^\pi=\frac{1}{2}$) keV. Summing corrections of 10% and 5%, respectively, were required for the crossover decays. The near equality of the stopover and crossover branches indicate that these levels have probable spin $J=(\frac{1}{2},\frac{3}{2})$. An additional level at 652 keV was found to decay by a 367-keV γ ray to the 285-keV level, but apart from its presence no other properties could be extracted.

A search was made for possible ground-state decays from levels observed in the coincidence data. Only the 39- and 144-keV levels were found to have such decays; all other levels could be limited to have <5% ground state branches. Figure 5 shows a proposed decay scheme for ^{79}Sr deduced from these data. Spectroscopic results are summarized in Table II.

B. ^{80}Y → ^{80}Sr decay

The only previous report of levels in ^{80}Sr was by Nolte *et al.*,[2] who used the ^{66}Zn(^{16}O, 2n)^{80}Sr reaction and observed three excited states whose yield curves were consistent with two particle evaporation. They also measured the half-life of the lowest state at 386 keV to be $T_{1/2}=44\pm6$ ps, which implied a very enhanced transition of $B(E2)=72\pm10$ W.u., indicating collective deformation.

The assignment of these γ rays to ^{80}Sr was confirmed by the cross bombardments indicated in Table I and by in-beam yield curves and γ-γ studies. The in-beam and radioactivity yield curves were compared to the predictions of the evaporation code CASCADE.[11] While the relative cross sections for isotope production were in only qualitative agreement with the code, the shapes of the experimental yield curves were reproduced very closely. The in-beam coincidence data allowed the observation of the ground state band up to $J^\pi=12^+$ and a sideband based on an 1142-keV state. These results will be reported separately.

In the radioactive decay of ^{80}Y the ground state band was populated up to spin $J^\pi=6^+$, together with five other states. A summed γ-γ coincidence spectrum for ^{80}Y lines is shown in Fig. 6. The decay half-life and total decay energy (Q_{EC}) of ^{80}Y were measured using the 386- and 595-keV lines, and these results were in good agreement with each other and are shown in Fig. 7. Apart from the 386-keV decay, no other ground-state branches were found. Levels at 1106 and 1268 keV originally suggested[5] to be in ^{80}Sr by our preliminary analysis were found to arise from summing effects. These levels are deleted from the proposed ^{80}Y

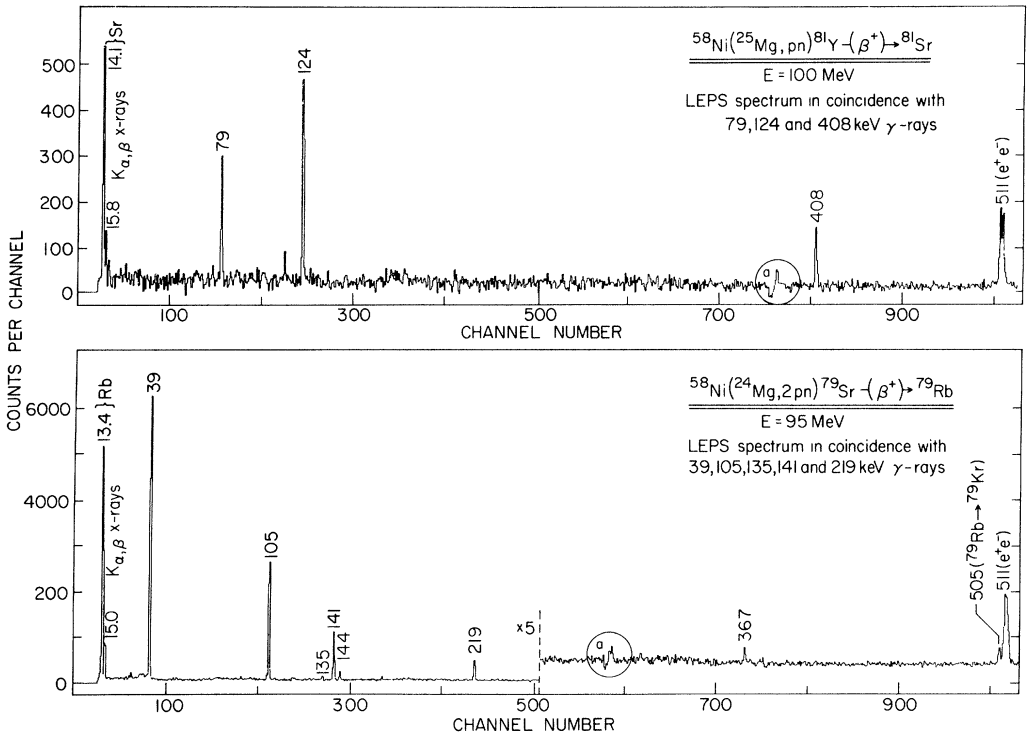

FIG. 4. Low-energy γ-ray spectra collected in coincidence with γ rays found only in ^{79}Rb (bottom) and ^{81}Sr (top). The circled features marked *a* arise from Compton backscattering between detectors.

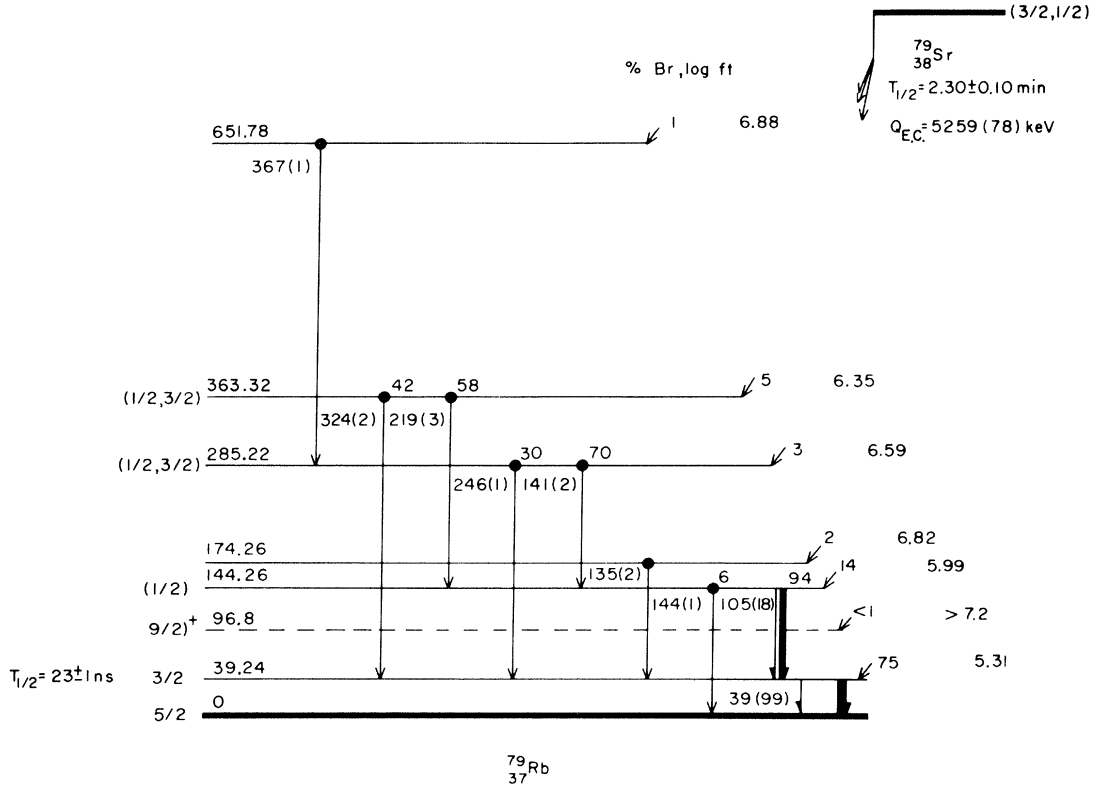

FIG. 5. The decay scheme of ^{79}Sr deduced from this work. The width of each arrow is proportional to total intensity; the dark area representing the unconverted fraction of the decay. The parity of the 39- and 144-keV levels is the same as the groung-state. Log*ft* values are calculated assuming there is no ground-state β^+ branch.

TABLE II. Summary of decay scheme information for ^{79}S, ^{80}Y, ^{81}Y, and ^{82}Y.

Parent isotope	E_X (keV)	E_γ (keV)	I_γ (arb)	I_{total} (arb)	BR%[f]	$J_i^\pi \rightarrow J_f^\pi$	Multipolarity	Logft[a]	$T_{1/2}$	α_k	Coincident transitions (keV)
^{79}Sr (2.30 ± 0.10 min)	39.24 ± 0.09	39.24 ± 0.09	100	99	100	$\frac{3}{2}^+ \rightarrow \frac{5}{2}^+$	$E2/M1$	5.31	23 ± 1 ns	4.1 ± 0.3	Rb($K\alpha, \beta$ x rays) 105, 135, 141, 219, 246, 324, and 367
	144.26 ± 0.07	104.99 ± 0.08	74	18	94 ± 2	$\frac{1}{2}^+ \rightarrow \frac{3}{2}^+$	$E2/M1$	5.99	< 7 ns	0.56 ± 0.24	Rb($K\alpha, \beta$ x rays) 39, 141, 219, 367
		144.30 ± 0.10	6[b]	1	6 ± 2	$\frac{1}{2}^+ \rightarrow \frac{5}{2}^+$	$E2$			0.29	141, 219
	174.26 ± 0.12	135.02 ± 0.10	12	2	100			6.82	< 7 ns		Rb($K\alpha, \beta$ x rays) 39
	285.22 ± 0.07	141.04 ± 0.08	15	2	70 ± 2			6.59	< 7 ns		Rb($K\alpha, \beta$ x rays) 39, 105, 144, 367
		245.93 ± 0.10	6[b]	1	30 ± 2						Rb($K\alpha, \beta$ x rays) 39
	363.32 ± 0.07	219.09 ± 0.09	21	3	58 ± 3			6.35	< 7 ns		Rb($K\alpha, \beta$ x rays) 39, 105, 144
		324.05 ± 0.10	15[b]	2	42 ± 3						Rb($K\alpha, \beta$ x rays) 39
	651.78 ± 0.13	366.56 ± 0.11	7	1	100			6.88			39, 105, 141
^{80}Y (33.8 ± 0.6 s)	385.87 ± 0.10	385.87 ± 0.10	100	100	100	$2^+ \rightarrow 0^+$[c]	$E2$	≥5.84	44 ± 6 ps[d]		Sr($K\alpha, \beta$ x rays) 595, 690, 756 783, 852, 1185, 1278, 1395
	980.93 ± 0.18	595.06 ± 0.15	43	42	100	$4^+ \rightarrow 2^+$	$E2$	5.38			Sr($K\alpha, \beta$ x rays) 386
	1142.35 ± 0.16	756.48 ± 0.13	11	11	100	$(2^+)_2 \rightarrow 2^+$	$E2/M1$	5.78			386
	1571.09 ± 0.18	1185.22 ± 0.15	15	15	100	$\rightarrow 2^+$		5.47			386
	1663.59 ± 0.30	1277.52 ± 0.29	3	3	100	$\rightarrow 2^+$		6.13			386
	1763.74 ± 0.18	782.81 ± 0.16	6	6	100	$6^+ \rightarrow 4^+$	$E2$	5.78			386, 595
	1780.42 ± 0.30	1394.55 ± 0.29	1	1	100	$\rightarrow 2^+$		6.55			386
	1832.83 ± 0.20	690.50 ± 0.25	3	3	27 ± 4	$(4^+)_2 \rightarrow (2^+)_2$	$E2$	5.44			386, 756
		851.90 ± 0.15	9	9	73 ± 4	$(4^+)_2 \rightarrow 4_1^+$	$E2/M1$				386, 595
^{81}Y (72.0 ± 1.5 s)	79.19 ± 0.05	79.19 ± 0.05	100	100	100	$\frac{5}{2}^- \rightarrow \frac{1}{2}^-$	$E2$	> 6.25	370 ± 85 ns		Sr($K\alpha, \beta$ x rays) 124, 408
	203.34 ± 0.10	124.15 ± 0.09	159	75	100	$(\frac{5}{7}^+, \frac{7}{2}) \rightarrow \frac{5}{2}^-$	$E1, E2/M1$	5.69	< 7 ns		Sr($K\alpha, \beta$ x rays) 79, 408
	203.34 + Δ	Δ + 50	< 2	41	100	$(+) \rightarrow (\frac{5}{2}^+, \frac{7}{2})$		5.25[e]	500 nsec < $T_{1/2}$ < 1 s		
	611.70 ± 0.15	408.36 ± 0.11	62	18	100	$(+) \rightarrow (\frac{5}{2}^+, \frac{7}{2})$		5.43	< 7 ns		Sr($K\alpha, \beta$ x rays) 79, 124
^{82}Y (9.5 ± 0.4 s)	573.68 ± 0.09	573.68 ± 0.09	100	96	100	$2^+ \rightarrow 0^+$	$E2$	5.14			602, 737
	1175.67 ± 0.10	602.14 ± 0.09	41	39	91 ± 1	$(2)^+ \rightarrow 2^+$	$E2/M1$	4.98			573
		1175.52 ± 0.15	4[b]	4	9 ± 1	$(2)^+ \rightarrow 0^+$	$E2$				
	1311.03 ± 0.14	737.35 ± 0.10	9	9	100	$0^+ \rightarrow 2^+$	$E2$	5.61			573

[a] Relative logft values are shown and were calculated assuming zero ground-state β^+ branches. The values for ^{80}Y and ^{81}Y are probably absolute, as parent and daughter have very different ground-state spins.

[b] Corrected for crossover summing.

[c] A concurrent in-beam study during the present work has established the ground-state band to $J \sim 12^+$.

[d] Reference 2, Nolte *et al.*, Z. Phys. A 268, 267 (1974).

[e] The Δ state is isomeric, and coincidence measurements give no indication of how it is populated. This ft value is a lower limit.

[f] Branching ratio for levels with more than one decay.

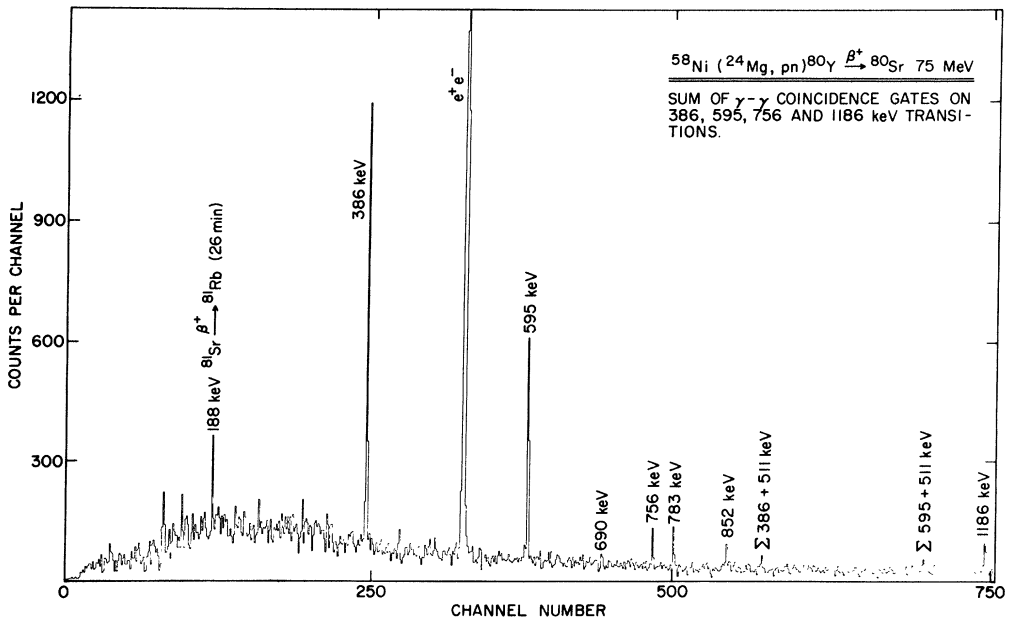

FIG. 6. A spectrum of γ rays from the decay of ^{80}Y, constructed by summing several coincidence gates from the γ-γ data.

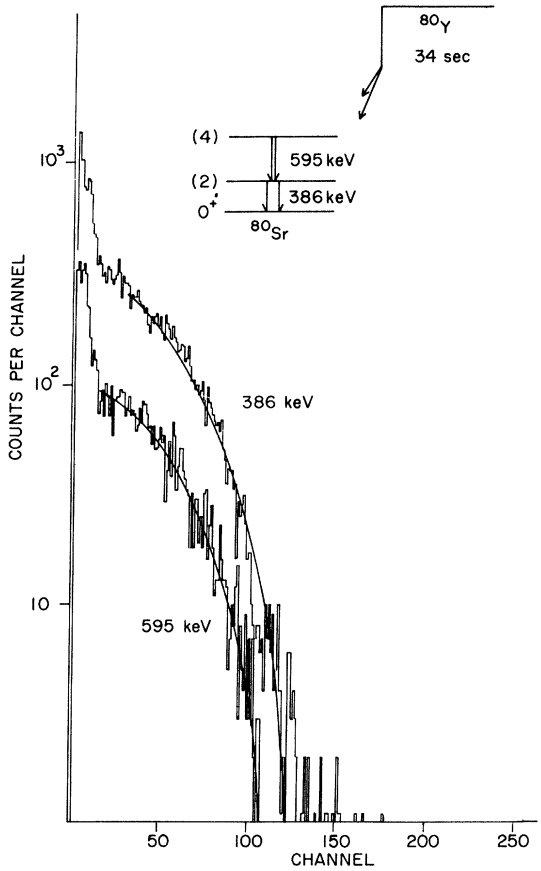

FIG. 7. The positron spectra in coincidence with the 386- and 595-keV decays in ^{80}Sr. The decay energy of ^{80}Y was deduced to be $Q_{EC}=6952\pm152$ keV.

decay scheme (Fig. 8). Table II summarizes the features of the ^{80}Y→^{80}Sr decay. The β branching to the 386-keV level may be considered an upper limit, as there was evidence of several other weak decays to this state. Apart from this, the strong β decays were to the $J^\pi=4^+$ member of the ground-state band and to the $J^\pi=(4^+)$ member of the side-band at 1832 keV. Consequently the most likely spin assignment for ^{80}Y is $J=4$, although rigorous proof must await further spectroscopic studies of ^{80}Sr.

C. ^{81}Y→^{81}Sr decay

This activity was identified by cross bombardments and yield curve measurements (Table I) and by the observation of intense Sr $K\alpha$, β x rays in coincidence with γ rays of this decay. The optimum production of ^{81}Y, relative to other isotopes, was found using the ^{58}Ni(^{25}Mg, pn)^{81}Y reaction at 100 MeV with a tape shuttle repetition rate of 52 sec. Three strong transitions were observed, of 79, 124, and 408 keV. The half-life for this new activity was measured to be 72.0 ± 1.5 s (124-keV line) and 70 ± 6 s (408-keV line). No evidence was found for the previously reported[3] 5-min activity attributed to ^{81}Y.

The three strong γ rays were mutually in coincidence, indicating a cascade. The ratios of their intensities were found to be quite different in the singles and coincidence data, which implied that one or more isomers were present. Coincidence timing measurements revealed that this was indeed

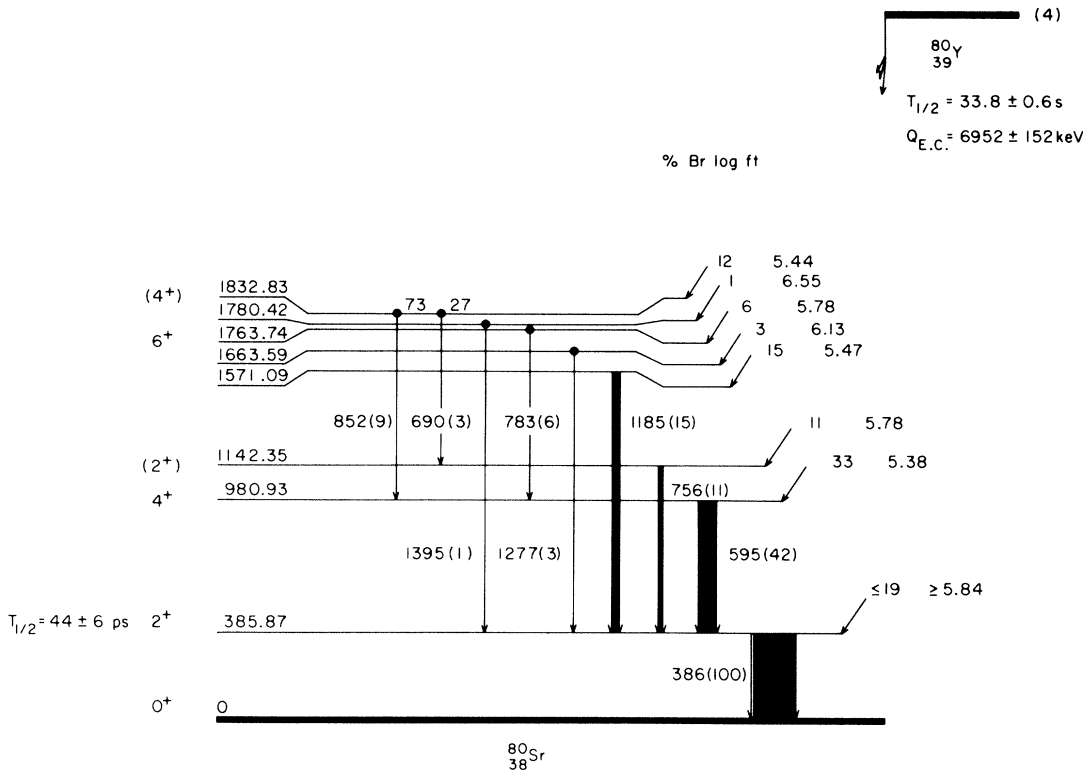

FIG. 8. The decay scheme of ^{80}Y deduced from this work.

the case. The 124- and 408-keV lines appeared promptly with the 511-keV signature of β^+ decay, and hence the levels from which these two γ rays originate have half-lives less than the electronic time resolution $T_{1/2} \leq 7$ ns. In contrast the 79-511-keV and 79-124-keV time spectra revealed an isomer with a half-life $T_{1/2} = 370 \pm 85$ ns, with the 79-keV transition occurring after the 124-keV transition. The 79-124-keV time spectrum is illustrated in Fig. 3.

^{81}Sr has a ground state spin and parity[17] of $J^\pi = \frac{1}{2}^-$. The earlier $J^\pi = \frac{9}{2}^+$ assignment of Ref. 4 has not been substantiated by the more recent in-beam spectroscopy[18] of ^{81}Rb. The isomeric half-life and singles intensities allow an assignment of $J^\pi = \frac{5}{2}^-$ for the 79-keV state in the following manner. To support the 124-keV γ intensity the 79-keV transition must be partially converted, with $\alpha_T > 0.67$. This eliminates the possibility of pure dipole decay as $\alpha_T^{79}(M1) = 0.30$ and $\alpha_T^{79}(E1) = 0.19$. The parity changing $M2/E1$ mixture may be eliminated since an $\alpha_T > 0.67$ requires $\delta > 0.22$ which, together with the isomeric half-life of 370 ns would imply an unrealistically large transition strength of $B(M2) > 37$ W.u. A similar argument for an $E2/M1$ mixture implies $\delta > 0.4$ and this leads to $B(M1) = 8 \times 10^{-5}$ W.u. and $B(E2) = 0.95$ W.u. While this possibility cannot be totally excluded, such an $M1$ transition would be one of the weakest observed[19] in the $A = 45$ to 90 region. A pure $M2$ decay of 79 keV would have $B(M2) = 315 \pm 72$ W.u., which leaves only the possibility that this is a pure $E2$ transition with $B(E2) = 6.8 \pm 1.6$ W.u.

Some restrictions can also be made on the spin and parity of the 203-keV level. Its prompt lifetime excludes decays with $\Delta J \geq 2$ as these would imply unrealistic transition strengths, and thus the spin and parity of this level is limited to $J^\pi = (\frac{3}{2}, \frac{5}{2}, \frac{7}{2})^\pm$. No evidence was found for a ground-state decay, to a limit of <3%, so the $\frac{3}{2}^\pm$ and $\frac{5}{2}^-$ hypotheses are unlikely. A measurement of the conversion of the 124-keV γ ray was deduced from a window set on the 408-keV transition in the X-γ coincidence data. After subtracting a contribution due to the K x rays from the converted part of the 79-keV transition, a conversion coefficient of $\alpha_K^{124} = 0.3 \pm 0.2$ was extracted. This coefficient is consistent with an $E2/M1$ transition, but the large uncertainty on this value does not allow the exclusion of an $E1$ decay. Consequently the 203-keV level can only be limited to have a spin/parity assignment of $J^\pi = (\frac{5}{2}^+, \frac{7}{2}^\pm)$.

Transitions observed in the decay of ^{81}Y are shown in the top panel of Fig. 4. Intense x rays

are seen in coincidence with the 79- and 124-keV lines, a feature which cannot be explained by the internal conversion of the three observed γ rays. Further, the number of coincident 511-keV transitions is not sufficient to balance the observed decay intensities. The total decay energy of ^{81}Y precludes dominant electron capture decay (estimated at <1%) so the presence of a second isomeric state appears probable. Some properties of the isomer may be extracted from the data. Limits on its lifetime come from the γ-γ coincidence experiment and the measurement of the ^{81}Y decay half-life. Because of the suppression of coincident 511-keV γ rays (and possibly other γ-ray transitions populating the upper isomer) by a factor of more than 12, the isomer must have $T_{1/2} > 500$ ns. In contrast, no deviation from a simple 72-s exponential decay curve was found for the 124-keV γ ray, although least-squares fits were performed which allowed two decay components and feeding through such an isomer. However, this latter fitting technique was rather insensitive to very short half-lives and only allowed a limit of $T_{1/2} < 10$ s to be set with confidence.

A careful search was made for a low energy ($E_\gamma < 124$ keV) γ-ray transition corresponding to the unconverted part of this postulated isomeric transition. No candidates were found, implying the total conversion coefficients of this transition is $\alpha_T \geq 20$.

A separate experiment was done to check for the possibility of isomers in ^{81}Sr with $T_{1/2} > 1$ s. Thick targets of natural zinc were irradiated by ^{18}O and ^{19}F beams which were mechanically chopped periodically and γ-ray spectra were collected during the "beam-off" periods. The Compton background was much higher in these spectra than in the He-jet experiments, and no indication of 79- or 124-keV γ rays were found. Gamma rays associated with the ^{81}Sr$\rightarrow^{81}$Rb decay were clearly seen, so ^{81}Sr nuclei were undoubtedly produced, and the ^{64}Zn(^{19}F, pn)^{81}Sr and ^{58}Ni(^{25}Mg, $2p$)^{81}Sr reactions are sufficiently similar so that it is unlikely that there are large differences in the relative population of high- and low-spin states. Consequently we have taken this as an indication that no long-lived isomers with $T_{1/2} > 1$ s exist in ^{81}Sr. This limits the possible half-life of this level to the range of 500 ns to 1 s.

The limitation of conversion coefficient ($\alpha_T \gtrsim 20$) and half-life (500 ns $< T_{1/2} <$ 1 s) restrict the decay of the upper isomer to be $\Delta J = 1$ or 2. These criteria are met by dipole decays of about 5 keV or quadrupole decays of less than 45 keV. The absence of a strong decay to the ground-state or to the 79-keV level favors a high-spin positive parity state. Certainly the low lying $J^\pi = \frac{7}{2}^+$ and $\frac{9}{2}^+$ isomers found in odd-A nuclei in this region would be good candidates for this level.

The final decay scheme deduced from these data (Table II) is shown in Fig. 9. Two independent mass measurements were made, in coincidence

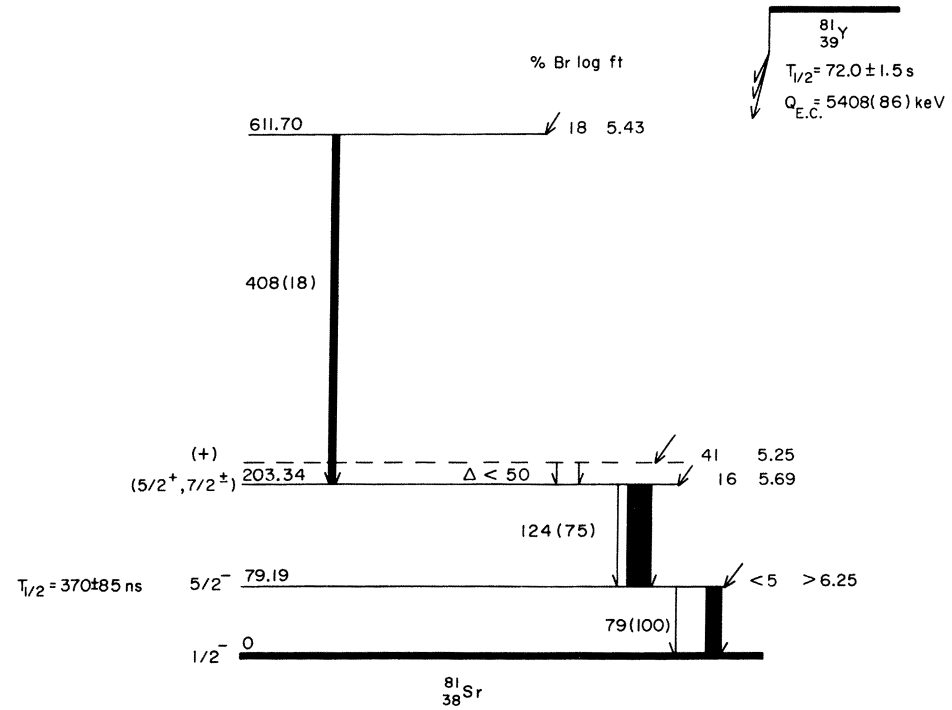

FIG. 9. The decay scheme for ^{81}Y. Only 80% of the population of the 79-keV isomer could be accounted for.

with the 124- and 408-keV γ rays (Table III). It will be noticed that the 79-keV total transition intensity is not balanced by the observed decays to it. This can be attributed, in part, to the long lifetime of the 79-keV level which hindered the observation of weaker transitions to this state, and to some uncertainty in the mixing ratio for the 124-keV level. The branching ratios and logft values were calculated assuming that the 79-keV intensity represented 100% of the β decays from ^{81}Y.

D. ^{82}Y → ^{82}Sr decay

The ^{82}Y → ^{82}Sr decay presents another case where levels in ^{82}Sr had been reported[2,20] from in-beam γ spectroscopy, but where the previously reported information[3] from the radioactive decay of ^{82}Y is not consistent with these data. We have produced ^{82}Y with ^{24}Mg beams on natural Ni targets, and have now found the γ rays associated with the de-excitation of ^{82}Sr levels reported from in-beam experiments. Subsequent confirmation of their assignments came from the absence of these γ rays when enriched ^{58}Ni targets were used, and the strong presence of the γ rays when using highly enriched ^{60}Ni targets.

The half-life (9.5 ± 0.4 s) and total decay energy (Table III) of ^{82}Y were measured using the 574-keV γ ray. The half-life result has been confirmed by another recent measurement of $T_{1/2}$ = 9.5 ± 0.5 s by Deprun *et al.*[7] and that of $T_{1/2} \approx 9$ s by the FSU group of Medsker *et al.*[21]

Four γ-ray transitions were seen, depopulating the first and second 2^+ states and the first-excited 0^+ level (Table II). Consequently a good candidate for the spin of ^{82}Y is $J^\pi = 1^+$ as has been reported[3] for the 4.6-s state in ^{84}Y. However, unlike ^{84}Y, no evidence was found in this work for a longer lived activity of about 10 min half-life which had been suggested in previous studies[22] employing off-line chemical separation and radioactivity decay genetic techniques.

IV. DISCUSSION

A. Nuclear level schemes

1. ^{79}Sr → ^{79}Rb decay

The ground-state spin of ^{79}Rb has been measured[16,23] to be $J = \frac{5}{2}$ by atomic beam measurements and this observation is supported by radioactivity studies.[24,25] However, conflicting parity assignments have been made in these reports. In order to interpret the results of this experiment, and also to understand recent in-beam results,[15,26] knowledge of the parity is vital as it reflects the difference between fp-shell and g-shell occupancy for the valence proton.

There is very little model-independent information available on the ground-state parity of ^{79}Rb.

TABLE III. Measured positron end points and Q_{EC} values for ^{79}Sr and $^{80-84}$Y.

Isotope	Gating transition (keV)	$E_{\beta^+}^{max}$ (keV)	Q_{EC} (keV)	Q_{EC} adopted (keV)	Q_{EC} previously reported (keV)
^{79}Sr	135	4065(120)	5621(120)		
	141	3952(104)	5258(104)	5259(78)	4930(120)[c]
^{80}Y	386	5554(306)	6968(306)		
	595	4945(175)	6948(175)	6952(152)	
^{81}Y	124	4235(112)	5460(112)		
	408	3701(135)	5333(135)	5408(86)	
^{82}Y	573	6273(185)	7868(185)	7868(185)	7620(100)[c]
^{83}Y	422	2868(85)	4571(85)[a]	4571(85)	4260(80)[c]
^{84}Y	793	4684(135)	6499(135)[b]		
	974+1040	2580(170)	6409(170)[b]	6464(106)	6950(30)[d]

[a] This measurement determines Q_{EC} for the low spin ($T_{1/2}$ = 2.85 min) isomer. Recent results of Deprun *et al.*[7] suggest the high spin isomer (7.10 min) is the ground state, having Q_{EC} = 4260 ± 80 keV and thus placing the low spin isomeric state at 311 ± 116 keV excitation.

[b] ^{84}Y is known to have both low- and high-spin positron decays, with half-lives of 4.6 sec and 39 min, respectively. Probable spins and parities are $J^\pi = 1^+$ and 5^-. These results show the two levels to be nearly degenerate and systematic trends suggest $J^\pi = 1^+$ for the ground state; in contrast these data slightly favor 5^-.

[c] Reference 7.

[d] Reference 36.

The magnetic moment has been measured[27] to be $\mu = 3.36 \pm 0.04$ nm which is not consistent with the Schmidt value for a single $1f_{5/2}$ proton. Consequently Ekstrom *et al.* assumed this implied $1g_{9/2}$ shell occupancy and assigned positive parity. This may not be a unique way of explaining this anomolously large moment. A parity assignment for ^{79}Rb from radioactive decay pivots on the parity of the 688-keV level in ^{79}Kr which is fed by 50% of the decay and has $\log ft = 4.9$. The only direct measurement of the 688 keV parity is the measurement of the internal conversion of this decay[17] ($\alpha_K = 4 \times 10^{-4}$) which implies positive parity for the 688-keV level and consequently also for ^{79}Rb. However, a measurement of such a small degree of conversion is difficult and systematic errors are hard to avoid. In summary, the direct evidence for the parity of ^{79}Rb favors a positive hypothesis, but is not definitive. An unambiguous assignment would be most valuable in understanding ^{79}Rb and neighboring nuclei. The present experiment has done little to clarify this difficult situation. The presence of the low-lying triplet of states with $J = \frac{5}{2}$, $\frac{3}{2}$, and $\frac{1}{2}$ in ^{79}Rb is reminicent of the other odd Rb isotopes with $N = 44$, 46, 48, and 50, where these levels have negative parity and have been associated with proton occupation of the $1f_{5/2}$, $2p_{3/2}$, and $2p_{1/2}$ shell model states. However, this is a transitional region, changing from closed shell behavior at $N = 50$, $Z = 40$ to rotational behavior near $N \approx Z \approx 40$. The even-even neighbors of ^{79}Rb are ^{78}Kr and ^{80}Sr. Both have been found to have collective bands consistent with an rms deformation of $|\beta| \sim 0.3$. Such a large deformation, either of positive or negative sign, has the effect of depressing certain $1g_{9/2}$ shell model states to a point where configurations of either positive or negative parity become equally probable. Consequently, it is difficult to deduce the parity of ^{79}Rb.

Despite this confused situation, the influence of the collective deformation is manifested in the observed $B(E2)$ transition strengths. In the $g_{9/2}$ decoupled band observed by Clements *et al.*[15] the Köln group[26] recently measured transition rates as high as $B(E2) = 137 \pm 28$ W.u. Amongst the lower spin states that were populated in radioactive decay we have measured $B(E2{:}\frac{3}{2} \rightarrow \frac{5}{2}) = 36 \pm 2$ W.u. and $B(E2{:}\frac{1}{2} \rightarrow \frac{3}{2}) > 30$ W.u., strengths which exceed those seen[3] between $\frac{3}{2}^-$ and $\frac{5}{2}^-$ states in heavier Rb isotopes by a factor more than 20. Additional spectroscopic studies of the ^{79}Rb levels, either via in-beam or radioactivity techniques, that could employ direct measurements of transition multipolarities from conversion electron spectroscopy would be of considerable help to clarify these difficulties.

2. $^{80}Y \rightarrow {}^{80}Sr$ decay

The observation of β branches from ^{80}Y to states in ^{80}Sr with spins as high as $J = 6$ indicates that ^{80}Y itself has a relatively high spin and thus no significant ground-state β decay branch should exist. This in turn implies that the calculated $\log ft$ values shown in Table II and Fig. 8 are absolute and can be used as a guide to limit the spin and parity of ^{80}Y. The two strongest β branches are to the two lowest $J^\pi = 4^+$ states and both have allowed $\log ft$ values of ~5.4 which determine the parity to be positive. In addition, the population of states with spins 2–6 indicates that the spin and parity of ^{80}Y is $J^\pi = 4^+$. This positive parity assignment is discussed in more detail in Sec. IV A 4.

The level scheme deduced from our data is shown in Fig. 8. It is being supplemented by in-beam spectroscopy studies using the ^{58}Ni(^{24}Mg, $2p$)^{80}Sr reaction. A preliminary investigation revealed the ground-state band to spin/parity $J^\pi = 12^+$, but the sidebands like those observed in ^{82,84}Sr (Refs. 23 and 36) were not strongly populated. Some initial calculations have been done using the IBA-1 code PHINT. The level scheme appears to correspond reasonably well to that predicted in the O(6) limit. The branching ratio of the upper 4^+ state was calculated to be $\mathrm{BR}(4_2^+ \rightarrow 2_2^+)/(4_2^+ \rightarrow 4_1^+) = 1.05$ in contrast to the experimental value of 0.37. However, no $4_2^+ \rightarrow 2_1^+$ branch was observed (<5% branch) which conforms with a selection rule ($\Delta\tau = 2$) in the O(6) limit. Candidates for the states at 1571 and 1663 keV are 3^+ and 3^-. The low-lying $J^\pi = 0^+$ state at 1000 keV reported by Alford *et al.*[28] was not reproduced by these calculations, the lowest $J^\pi = 0^+$ state being predicted to lie at 2.0 MeV. This anomalously low 0^+ state has been observed[20,29] in other Sr and Kr isotopes and is though to be an intruder state.

3. $^{81}Y \rightarrow {}^{81}Sr$ decay

The decay of ^{81}Y differs from that of the other odd neutron deficient Y isotopes in that it only has one β^+ decaying state, not two. $^{83\text{-}91}$Y all have $J^\pi = \frac{1}{2}^-$ ground-states with $J^\pi = \frac{9}{2}^+$ excited states which are β^+ decaying isomers.[3] Transfer reaction studies leading to $^{85\text{-}89}$Y (Refs. 30 and 31) show these states to have rather pure $2p_{1/2}$ and $1g_{9/2}$ shell model configurations, exhausting >60% of their sum rule transfer strengths. This supports the simple description of the Y isotopes ($Z = 39$) as having $2p_{1/2}$ ground-state with a first-excited state arising from promotion of the valence proton into the $1g_{9/2}$ shell. In Fig. 10 the relative positions of these states are shown. The information on levels in ^{83}Y comes from the mass measurements made in this work, and that of the

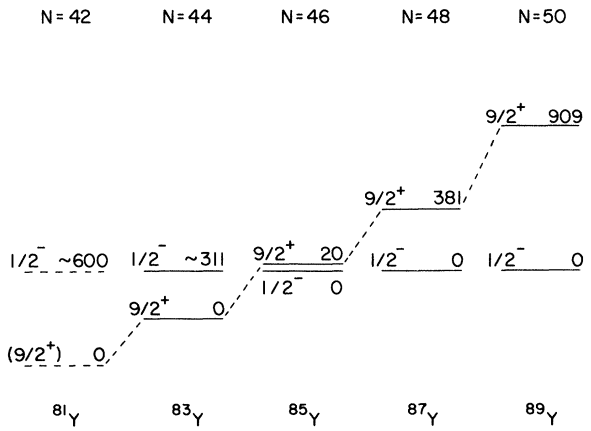

FIG. 10. The systematic behavior of the first $J^\pi = \frac{1}{2}^-$ and $J^\pi = \frac{9}{2}^+$ states in the odd yttrium isotopes. The excitation energy of the $\frac{1}{2}^-$ state in ^{83}Y has been measured to be 311 ± 116 keV by positron end point measurements (see Table III). The position of the states in ^{81}Y is by extrapolation, but is supported by the observed β feeding of high spin positive parity levels in ^{81}Sr.

Orsay group (see Table III). It can be seen that if ^{81}Y follows the trend evident amongst the other isotopes a $J^\pi = \frac{9}{2}^+$ ground-state may be expected with a $J^\pi = \frac{1}{2}^-$ state at ~600 keV. This trend can be explained in the framework of the Nilsson[32] model for a system changing from spherical behavior at the $N = 50$ neutron shell closure to oblate deformed behavior at $N = 40$. In this shape transition the $g_{9/2}$ ($J = \frac{9}{2}$) and $P_{1/2}$ orbits cross at $\beta \sim -0.1$ and ^{81}Y may thus be expected to have a ground-state deformation of $\beta \sim -0.15$. If this is so then $\frac{7}{2}^+$ and $\frac{5}{2}^+$ levels are expected below 600 keV, so the $\frac{1}{2}^-$ state can decay by γ, rather than β, emission. This prediction conforms with the observed single β^+ decay found for ^{81}Y.

The systematics of the odd neutron Sr isotopes show a trend similar to that observed among the Y isotopes, $^{83\text{-}87}$Sr have $J^\pi = \frac{7}{2}^+$ or $\frac{9}{2}^+$ ground states with low lying $J^\pi = \frac{1}{2}^-$ isomers.[3] In ^{81}Sr the position of the configurations is reversed resulting in a $J^\pi = \frac{1}{2}^-$ ground state.[17] The levels at 203 and 203 + Δ keV are good candidates for a closely spaced $\frac{7}{2}^+$, $\frac{9}{2}^+$ doublet similar to the ground and first excited states in ^{83}Sr.

The odd-N nuclei also show strong isotonic trends in this region. ^{81}Sr fits readily into the $N = 43$ and 45 systematics. However, it differs from its neighboring $N = 43$ isotones in that the $\frac{5}{2}^-$ level is depressed below the $\frac{7}{2}^+$, $\frac{9}{2}^+$ doublet which prevents these states both being isomeric. The decrease in excitation energy of the $\frac{5}{2}^-$ state is regular with increasing Z and may lead to the $Z = 40$, $N = 43$ nucleus ^{83}Zr having a $\frac{5}{2}^-$, rather than $\frac{1}{2}^-$, ground-state spin. The $B(E2{:}\frac{5}{2}^- \rightarrow \frac{1}{2}^-)$ value for the $N = 43$ isotopes has a value[3] of 2.12 W.u. in ^{77}Se, 3.49 W.u. in ^{79}Kr, and 7.49 W.u. in ^{81}Sr, an increase which may reflect the increase of collectivity of all states as one approaches $N \approx Z \approx 40$.

4. ^{82}Y → ^{82}Sr decay

The β^+ decay of ^{82}Y is by transitions to states with spin and parity 2^+ and 0^+. The logft values, when calculated assuming zero ground-state β branch (Table II), are significantly lower than allowed transitions in neighboring nuclei. This is probably an indication of sizeable (≈50%) decay branch to the ^{82}Sr ground state which itself would be an allowed transition with log$ft = 4.9$. Consequently, although the ground-state branch was not observed in this work, we can confidently make a spin and parity assignment for ^{82}Y as $J^\pi = 1^+$. The positive parity assignment is consistent with the trend observed across the odd-odd Y isotopes, with the more neutron deficient having positive parity ground-states (arising from both valence proton and neutron occupying $g_{9/2}$ shell orbits) and the stable and near stable isotopes having negative parity ground-states (arising from fp shell proton occupancy). This trend is consistent with that observed between the odd Y isotopes and which has been discussed in the previous section.

B. Nuclidic masses

In addition to the nuclear structure information which was obtained from the decay of ^{79}Sr and $^{80\text{-}82}$Y and described above, the measurement of the decay energies (Q_{EC}) of these nuclides can be of considerable use for delineation of the features of the nuclidic mass surface. This can be done in several instructive and informative ways: (1) direct comparison for each decay of the measured Q_{EC} values to predictions of the available mass models can be used to identify which models are more successful in this region; (2) conversion of the decay energy measurement to absolute mass excesses (using the accurately known[33] mass excesses of the light Rb isotopes, which are daughters of ^{79}Sr or granddaughters of $^{80\text{-}82}$Y) can also be used to provide direct comparison to model predictions, complementing the first difference comparisons afforded by the Q_{EC} data; (3) examination of variations in mass-related properties such as single-nucleon and two-nucleon separation energies and additional quantities derived from them, to identify and highlight systematic variations in the mass surface for $N \approx Z \approx 40$.

Figure 11 shows comparisons of the differences, Δ, between measured and predicted Q_{EC} values for ^{79}Sr and $^{80\text{-}82}$Y. Each arrow in the figure is labeled

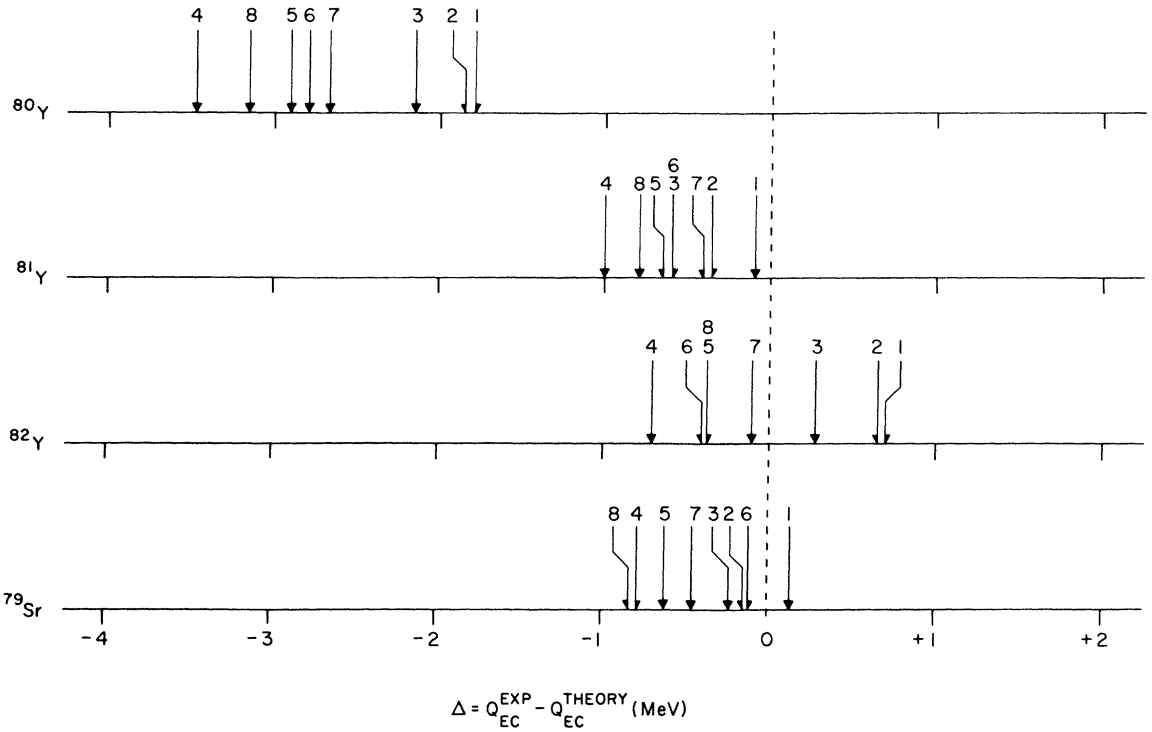

FIG. 11. Comparison of differences Δ between predicted and measured Q_{EC} for ^{79}Sr, ^{80}Y, ^{81}Y, and ^{82}Y. Numbers above the arrows identify individual mass models. From Ref. 34: 1 =Myers; 2 =Groote *et al.*; 3 =Seeger and Howard; 4 =Liran and Zeldes; 5 =Janecke, Garvey-Kelson; 6 =Comay and Kelson; 7 =Janecke and Eynon. From Ref. 35: 8 =Monahan and Serduke.

by a number corresponding to the Δ value obtained from the difference between the measured Q_{EC} of the particular isotope and predictions from the models.[34,35] For the four isotopes shown, one might expect that the various Δ values would be normally distributed with a mean close to zero, indicating the anticipated spread in predictions for Q_{EC} which come from mass models which contain many diverse features. While the expectation is well satisfied for ^{79}Sr and ^{82}Y, the most striking feature of Fig. 11 is of a significant discrepancy between calculated and experimental values of Q_{EC} for ^{81}Y and a much greater one for ^{80}Y. For the latter cases the measured decay energies are ~2–3.5 MeV less than predicted. Table IV shows mass excess values for ^{79}Sr and $^{80\text{-}82}$Y that were calculated from the reported mass excesses[26] of $^{79\text{-}82}$Rb by addition of the decay energy of ^{79}Sr, and the decay energies[28,36] for Sr and Y isotopes for $A = 80$ to 82. These results, when compared with mass excess predictions from the models, are summarized in Fig. 12 in the same manner as Fig. 11. There is a remarkable similarity between these two sets of data. Mass excesses for ^{79}Sr and ^{82}Y are predicted adequately, as were the Q_{EC} for these nuclides as noted above. For ^{80}Y,

TABLE IV. Computed mass excesses for ^{79}Sr, ^{80}Y, ^{81}Y, and ^{82}Y.

Isotope	Rb mass excess[a] (MeV)	Strontium Q_{EC} (MeV)	Yttrium Q_{EC}[b] (MeV)	Resultant mass excess (MeV)
^{79}Sr	−70.86(11)	5.26(8)[b]		−65.60(13)
^{80}Y	−72.19(2)	1.91(3)[c]	6.95(15)	−63.33(16)
^{81}Y	−75.45(4)	4.00(3)[d]	5.41(9)	−66.04(10)
^{82}Y	−76.21(2)	0.21(2)[d]	7.87(19)	−68.13(20)

[a] Reference 33.
[b] Present work.
[c] Computed from data of Ref. 28.
[d] Reference 36.

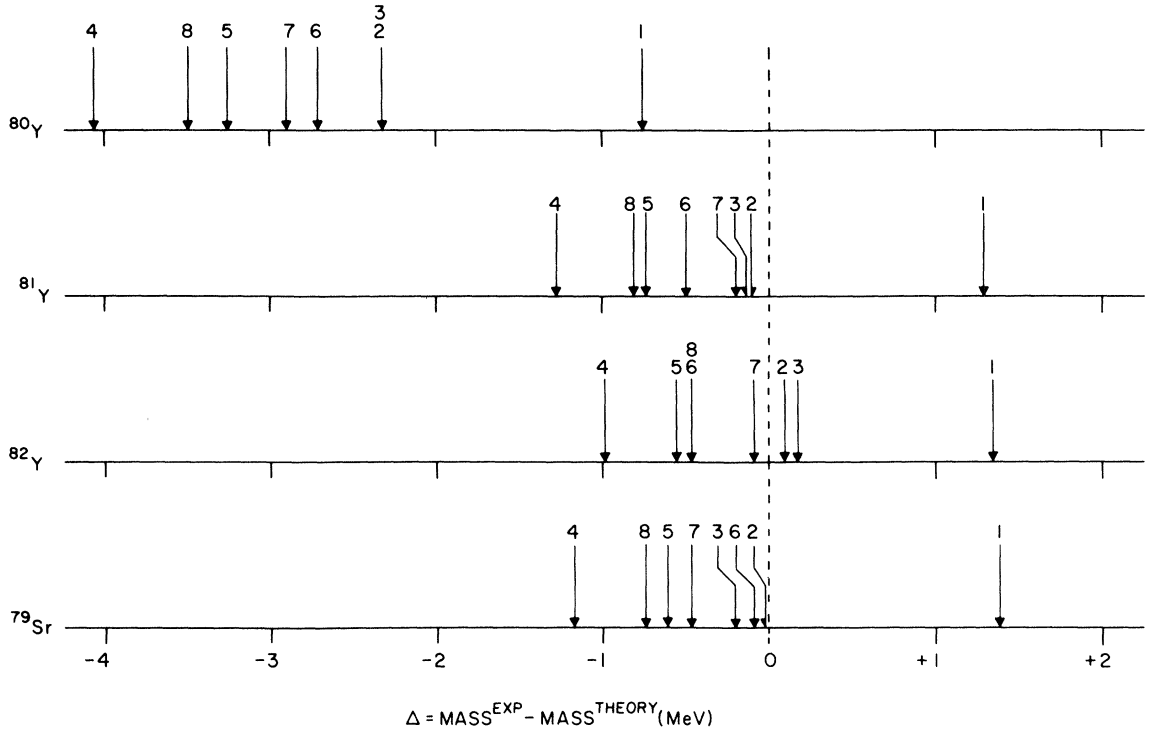

FIG. 12. Comparison of differences Δ between predicted and inferred mass excesses for ^{79}Sr, ^{80}Y, ^{81}Y, and ^{82}Y. Numbers above the arrows identify individual mass models as in Fig. 11.

the Δ values are again negative and large, spanning an even greater range than those for Q_{EC}. It is also noteworthy that there is a general self-consistency in the predictions. In both the Q_{EC} and mass excess comparison the rank ordering of the models by sign and magnitude of Δ is generally the same for the four nuclides. At the extremes are the models of Myers (labeled 1) and of Liran and Zeldes (labeled 4).

It is frequently the case that certain mass related properties such as single-nucleon and two-nucleon separation energies provide sensitive indications of systematic features of the nuclidic mass surface when these quantities are examined over long isotopic, isotonic, or isobaric chains. Figures 13 and 14 show the variations in five of these quantities: single-proton (S_p), two-proton (S_{2p}), single-neutron (S_n), two-neutron (S_{2n}) separation energies, and [S_n and $S_{2n}/2$] for the yttrium isotopes. The points for $^{80\text{-}82}$Y were computed from the mass excess data of Table IV; data for the heavier isotopes were obtained from the tabulation of Wapstra and Bos.[36] Both the S_p and S_{2p} plots show the gradual decrease in proton binding energy across the $A=80$ to $A=98$ mass range. It appears, however, that there is a small increase at ^{80}Y. Extrapolation of plots of this type to zero binding, without the ^{80}Y point would suggest that the proton drip line would occur at about $A=76$. The break in the trend at $A=80$ (as well as the large deviation between measured and predicted decay energies for ^{80}Y and ^{81}Y) implies that the drip line is likely to occur farther out. The plots of S_n and S_{2n} show additional irregular behavior. The S_n plot exhibits the normal odd-even oscillations and a jump at the $N=50$ neutron shell closure. A slight damping of the oscillations occurs at ^{81}Y. This is more apparent in the S_{2n} plot, where the odd-even oscillations are filtered out. The gradual increase in neutron binding energy across this mass range can be normalized by examination of the quantity [S_n and $S_{2n}/2$]. Here again one notices the change in the normal trend for the lightest Y isotopes.

The large discrepancy between the experimentally determined decay energy of ^{80}Y (and the ^{80}Y mass excess inferred from it) and the predictions of these quantities from the more recent mass tabulations is a major feature of this work. As summarized in Figs. 11 and 12, ^{79}Sr and ^{82}Y are slightly more bound than expected and the data for ^{81}Y and ^{80}Y show that this effect of increasing binding becomes more pronounced for these nuclides.

A full scale analysis of the features of the various mass models that might be performed using

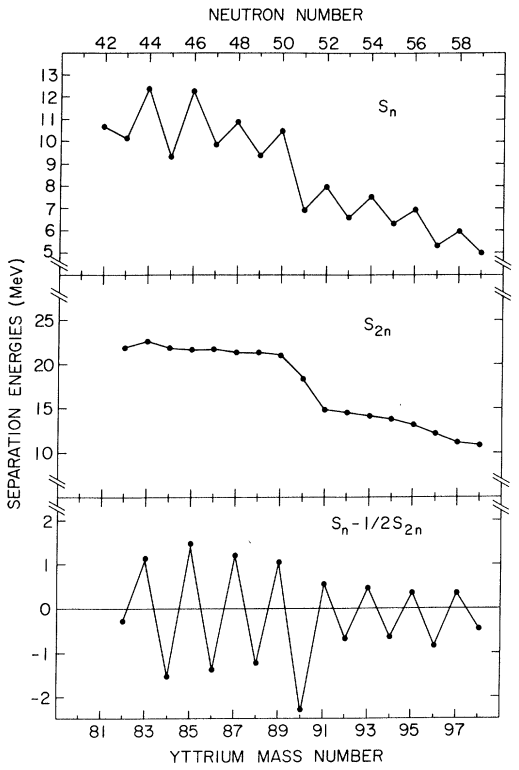

FIG. 13. Variation of single-neutron separation (top) S_n, two-neutron separation S_{2n} (middle), and neutron pairing ($S_n - \frac{1}{2} S_{2n}$) (bottom) energies across the Y isotopes. Results from the present work ($^{80-83}$Y) were combined with data from Ref. 36 for the heavier Y isotopes.

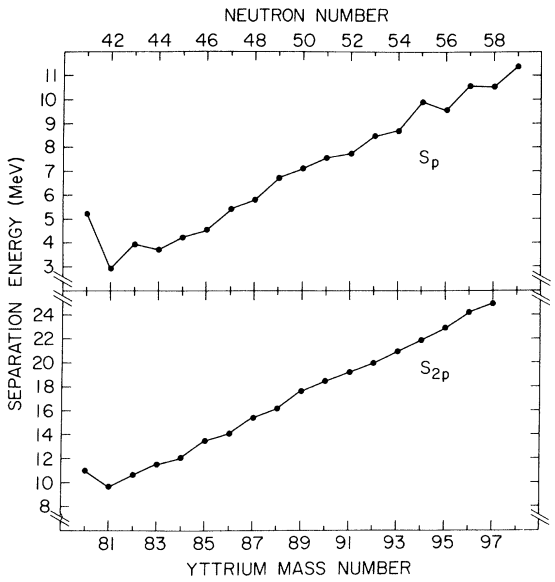

FIG. 14. Variation of single-proton separation S_p (top) and two-proton separation S_{2p} (bottom) energies across the Y isotopes. Results from the present work ($^{80-83}$Y) were combined with data for heavier Y isotopes and data for Sr and Rb nuclides from Ref. 36.

the ^{79}Sr and $^{80-82}$Y data to examine the reasons for these trends is beyond the scope of the present work. A more limited analysis, however, is possible for a subset of the models, those whose predictions are based on mass equations and relationships of the Garvey-Kelson type. In these models the observation of the approximate cancellation of residual interactions in various mass operator expressions leads to the use of the transverse (T) and longitudinal (L) relationships as predictive tools to estimate the mass of a particular isotope from the masses of neighboring nuclides.

Using this technique we have computed masses for ^{79}Sr and $^{80-82}$Y from the T relationship and mass data from Ref. 36 or results from the present work wherever they supersede the older results. The results of this calculation are shown in Table V. The upper portion shows the experimental

TABLE V. Experimental mass excesses (in MeV) for ^{79}Sr and $^{80-82}$Y and theoretical predictions from mass models which employ extrapolation procedures of the Garvey-Kelson type or variations thereof.

Isotope	Mass	Revised prediction (T relation)	Jänecke, Garvey-Kelson[a]	Comay and Kelson[a]	Jänecke and Eynon[a]	Monahan and Serduke[a]
^{79}Sr	−65.60(13)	−65.53	−64.99	−65.52	−65.14	−64.86
^{80}Y	−63.33(16)	−61.48	−60.18	−60.73	−60.54	−59.95
^{81}Y	−66.04(10)	−65.67	−65.30	−65.64	−65.84	−65.22
^{82}Y	−68.13(20)	−67.96	−67.57	−67.66	−68.04	−67.65
		Difference (experiment to theory)				
^{79}Sr		−0.07	−0.61	−0.08	−0.46	−0.74
^{80}Y		−1.85	−3.15	−2.60	−2.79	−3.38
^{81}Y		−0.37	−0.74	−0.50	−0.20	−0.82
^{82}Y		−0.17	−0.56	−0.47	−0.09	−0.48
	$\langle\Delta\rangle$:	−0.62	−1.27	−0.91	−0.89	−1.36
	Δ_{rms}:	0.95	1.67	1.35	1.42	1.80

[a] Reference 34.

masses for ^{79}Sr and $^{80-82}$Y and the masses as calculated from the T relationship. The four remaining columns list the mass predictions based on earlier Garvey-Kelson type extrapolations or variants thereof. The lower portion displays differences between experiment and theory, with average and root-mean-squared deviations summarized at the bottom. One notes that the difference between the revised predicted masses for ^{80}Y and the experimental result is approximately half that from earlier predictions. There are similar but less dramatic improvements for the other three nuclides as well. However, it is noteworthy that the ^{80}Y mass excess prediction, although improved in the revised calculation, is still significantly different from experiment. Clearly the noncancellation of the residual interaction components of the T operator is important. In other situations this feature has usually signaled the onset of an important new feature of nuclear structure and its influence on the mass surface.

The suggestion that the mass region around $N=40$, $Z=40$ is one characterized by rapid changes in nuclear deformation raises the question of the influence of this property on the masses of nuclides in this region. The neutron-deficient Rb isotopes, whose masses have been determined[33] down to $A=74$, span part of this region of deformation change, although the magnitude of the effects as signaled by the $2^+ \rightarrow 0^+$ energy spacing in the neighboring Sr and Kr isotopes is smaller as one proceeds away from $N=40$ and $Z=40$. Comparison of the differences between experimental and predicted masses[34,35] for the light Rb isotopes show trends similar to Figs. 11 and 12, although no single Rb case displays quite the same magnitude as seen for ^{80}Y.

V. SUMMARY

The present work has resulted in the identification of a new neutron-deficient nuclide, ^{80}Y. Extensive decay scheme information has been obtained for ^{80}Y and the previously poorly characterized radioactivities of ^{79}Sr, ^{81}Y, and ^{82}Y. In general, the properties of these nuclei, as inferred from previous in-beam studies of level schemes and transition probabilities and the present radioactivity investigations, can be interpreted as arising from the influence of large oblate nuclear deformation in this mass region $\beta \sim 0.3$. Within the framework of the interacting-boson-approximation (IBA) model, the low lying level structure of ^{80}Sr can be reproduced through calculations which place ^{80}Sr at or near the O(6) limit of the IBA model. Decay energy and mass measurements for ^{79}Sr and $^{80-82}$Y show progressively larger deviations from theoretical predictions as one approaches $N \approx 40$, $Z \approx 40$. This feature parallels the increase in nuclear deformation in this region and may be the signature of the influence of the nuclear deformation of these isotopes on the mass surface.

ACKNOWLEDGMENTS

The authors wish to acknowledge the help of the BNL Tandem Van de Graaff laboratory staff for computer assistance, target preparation, and for providing the heavy-ion beams used in this investigation. We are indebted to L. Medsker and Y. LeBêyec for valuable information prior to publication from their radioactivity studies in the mass 80 region. Assistance from R. Casten in performing the IBA model calculations for ^{80}Sr is gratefully acknowledged. This research has been performed under Contract No. DE-AC02-76 CH00016 with the Division of Basic Energy Sciences, U. S. Department of Energy.

---

*Present address: Shuster Laboratory, Department of Physics, University of Manchester, Manchester, M13-9PL, England.

[1]Proceedings of the 3rd International Conference on Nuclei far from Stability, Cargèse, France, 1976, CERN Report No. 76-13, 1976 and references therein.

[2]E. Nolte, Y. Shida, W. Kutschera, R. Prestle, and H. Morinaga, Z. Phys. A 268 267 (1974).

[3]See, for example, *Table of Isotopes*, 7th ed., edited by C. M. Lederer and V. S. Shirley (Wiley, New York, 1978).

[4]T. A. Doran and M. Blann, Nucl. Phys. A161, 12 (1971).

[5]P. E. Haustein, C. J. Lister, D. E. Alburger, and J. W. Olness, *Atomic Masses and Fundamental Constants 6*, edited by J. A. Nolen and W. Benenson (Plenum, New York, 1980) p. 475.

[6]L. H. Fry, J. S. Clements, L. V. Theisen, and L. R. Medsker, Bull. Am. Phys. Soc. 24, 826 (1979).

[7]C. Deprun, S. Della Negra, J. P. Husson, H. Gaovin, and Y. Lebéyec, Z. Phys. A 295, 103 (1980).

[8]A. N. Bilge and G. G. J. Boswell, J. Inorg. Nucl. Chem. 33, 2251 (1974).

[9]A. N. Bilge and G. G. J. Boswell, J. Inorg. Nucl. Chem. 33, 4001 (1974).

[10]I. M. Ladenbauer-Bellis, H. Bakhru, and B. Jones, Can. J. Phys. 50, 3071 (1972).

[11]F. Pühlhoffer, Nucl. Phys. A280, 267 (1977).

[12]D. E. Alburger and T. G. Robinson, Nucl. Instrum.

Methods 164, 507 (1979).
[13]R. C. Pardo, C. N. Davids, M. J. Murphy, E. B. Norman, and L. A. Parks, Phys. Rev. C 15, 1811 (1977); C. N. Davids, G. A. Gagliardi, M. J. Murphy, and E. B. Norman, *ibid.* 19, 1469 (1979).
[14]C. J. Lister, P. E. Haustein, D. E. Alburger, and J. W. Olness, Bull. Am. Phys. Soc. 24, 828 (1979).
[15]J. S. Clements, L. R. Medsker, L. H. Fry, L. V. Thiesen, and L. A. Parks, Phys. Rev. C 20, 164 (1979).
[16]F. Rösel, H. M. Fries, K. Alder, and H. C. Pauli, At. Nucl. Data Tables 21, 91 (1978).
[17]R. Broda, A. Z. Zrynkiewicz, J. Stycén, and W. Walus, Nucl. Phys. A216, 493 (1973).
[18]H-G. Friedierichs, A. Gelberg, B. Heitz, K. O. Zell, and P. von Brentano, Phys. Rev. C 13, 2247 (1976).
[19]P. M. Endt, At. Data Nucl. Data Tables 23, 547 (1979).
[20]A. Dewald, U. Karp, W. Gast, A. Gelberg, K. O. Zell, and P. von Brentano, *Proceedings of the International Conference on Nuclear Physics, Berkeley, California, 1980,* LBL Report No. 11118, Vol. 1, p. 306.
[21]L. Medsker, private communication.
[22]V. Maxia, W. H. Kelly, and D. J. Horen, J. Inorg. Nucl. Chem. 24, 117 (1962); F. D. Buttement and G. B. Briscoe, *ibid.* 25, 151 (1962).
[23]C. Ekström, S. Ingelman, G. Wanberg, and M. Skarestad, Proceedings of the International Conference on Nuclei far from Stability, Cargèse, France, 1976, CERN Report No. 76-13, 1976, p. 193.
[24]J. Liptak and J. Kristiak, Nucl. Phys. A311, 421 (1978).
[25]E. W. Lingeman, F. W. N. DeBoer, P. Koldewijn, and P. R. Maurenzig, Nucl. Phys. A160, 630 (1971); R. Broda *et al.*, Acta Phys. Pol. B3, 263 (1972).
[26]J. Panqueva, H. P. Hellmeister, F. J. Bergmeister, and K. P. Lieb, *Proceedings of the International Conference on Nuclear Behavior at High Angular Momentum, Strasbourg, France, 1980,* p. 29.
[27]C. Ekström, S. Ingelman, G. Wannberg, and M. Skarestad, Nucl. Phys. A311, 269 (1978).
[28]W. P. Alford *et al.*, Nucl. Phys. A330, 77 (1979).
[29]A. Dewald, W. Gast, A. Gelberg, H-W. Schuch, K. O. Zell, and P. von Brentano, *Proceedings of the International Conference on Nuclear Behavior at High Angular Momentum, Strasbourg, France, 1980,* p. 33.
[30]L. R. Medsker, G. S. Florey, H. T. Fortune, and R. M. Weiland, Phys. Rev. C 12 1452 (1980).
[31]J. L. Horton and C. E. Hollandsworth, Phys. Rev. C 13, 2212 (1980).
[32]See, for example, A. Bohr and B. Mottelson, *Nuclear Structure* (Benjamin, New York, 1975), Vol. II, Chapter 5.
[33]M. Epherre *et al.*, Phys. Rev. C 19, 1504 (1979).
[34]S. Maripuu, At. Data Nucl. Data Tables 17, 410 (1976).
[35]J. E. Monahan and F. J. D. Serduke, Phys. Rev. C 17, 1196 (1977).
[36]A. H. Wapstra and K. Bos, At. Data Nucl. Data Tables 19, 175 (1977).